

Developments of highly-multiplexed, multi-chroic pixels for Balloon-Borne Platforms

F. Aubin^a, S. Hanany^a, B. R. Johnson^b, A. Lee^c, A. Suzuki^{c,d}, B. Westbrook^c, and K. Young^a.

the date of receipt and acceptance should be inserted later

Abstract We present our work to develop and characterize low thermal conductance bolometers that are part of sinuous antenna multi-chroic pixels (SAMP). We use longer, thinner and meandered bolometer legs to achieve 9 pW/K thermal conductance bolometers. We also discuss the development of inductor-capacitor chips operated at 4 K to extend the multiplexing factor of the frequency domain multiplexing to 105, an increase of 60% compared to the factor currently demonstrated for this readout system. This technology development is motivated by EBEX-IDS, a balloon-borne polarimeter designed to characterize the polarization of foregrounds and to detect the primordial gravity waves through their B -mode signature on the polarization of the cosmic microwave background. EBEX-IDS will operate 20,562 transition edge sensor bolometers spread over 7 frequency bands between 150 and 360 GHz. Balloon and satellite platforms enable observations at frequencies inaccessible from the ground and with higher instantaneous sensitivity. This development improves the readiness of the SAMP and frequency domain readout technologies for future satellite applications.

Keywords Balloon-borne, bolometer, sinuous antenna multi-chroic pixels, frequency domain multiplexing readout.

1 Introduction

The recent combined results from *Planck* and BICEP2 have shown that in order to detect the signature of primordial gravity waves as B -modes on the cosmic microwave background (CMB), the Galactic foregrounds must be thoroughly understood [1]. The E and B Experiment - Inflation and Dust Surveyor (EBEX-IDS) is a balloon-borne polarimeter designed to achieve such detection and characterization. EBEX-IDS will re-use the attitude control system and most hardware components from EBEX to mitigate operational risks. Due to the lower density of atmosphere at float, the power absorbed by the detectors is at least a

^a School of Physics and Astronomy, University of Minnesota, Minneapolis, MN 55455, USA;

^b Department of Physics, Columbia University, New York, NY, 10027, USA;

^c Department of Physics, University of California, Berkeley, Berkeley, CA 94720, USA;

^d Lawrence Berkeley National Lab, Berkeley, CA 94720, USA;

E-mail: faubin@umn.edu

factor of 10 smaller compared to ground-based telescopes and is dominated by the instrument. The 1.5 m aperture Gregorian Mizuguchi-Dragone telescope will be composed of an ambient temperature primary mirror and two additional mirrors cooled to 4 K to minimize instrument load on the detectors; see Figure 1. The scanned patch will be shared with ground-based experiments such as POLARBEAR/Simons Array and BICEP2/Keck Array to improve the combined sensitivity while taking advantage of the deep coverage of these ground-based experiments and the high frequency coverage of the balloon-platform. EBEX-IDS will observe the sky in 7 different frequency bands from 150 to 360 GHz.

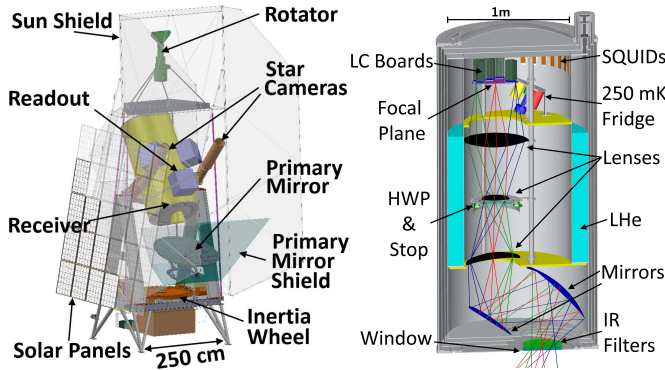


Fig. 1 *Left*: model of the EBEX-IDS gondola. *Right*: cut-through of a model of the EBEX-IDS cryostat.

We achieve polarization sensitivity by re-using the EBEX sapphire half-wave plate in combination with polarization sensitive sinuous antenna multichroic pixels (SAMP), a technology already deployed by the ground-based telescopes POLARBEAR2 and SPT-3G. EBEX-IDS will operate 20,562 bolometers divided into 3,427 tri-chroic SAMPs. To read out these detectors, we will use frequency domain multiplexing (FDM) readout with a multiplexing factor of 105 which will dissipate 1.3 kW of power. Increasing the multiplexing factor is essential for limiting the power dissipation. We will cool the electronic boards with liquid coolant reaching the field programmable gate arrays (FPGA) in thermal contact with 6.7 m² of radiator panels.

In this paper, we discuss the challenges and progress to develop these pixels for balloon-borne platforms. We develop low thermal conductance bolometers for optimal operation where 0.6 pW of power is expected to be absorbed by the bolometers at 150 GHz. We also increase the multiplexing factor of the FDM technology to 105, the highest multiplexing factor for the FDM to date, to achieve the desired sensitivity.

2 Low Thermal Conductance Detector Development

The SAMP shown in Figure 2 is fabricated with a series of sputter, plasma-enhanced chemical vapor deposition (PECVD), and evaporation thin film deposition steps, each patterned with stepper and/or contact lithography. Each metallic broadband sinuous antenna absorbs the incident light focused by an individual alumina lenslet. We are developing a new anti-reflection coating method with thermal spray to maximize transmission [2]. The antenna is composed of two perpendicular pairs of arms which are each sensitive to one polarization of

light. Niobium microstrips over silicon nitride couple the antennas to band-defining Dolph-Chebyshev filters and to manganese doped aluminium transition edge sensors (TES) via a titanium termination resistor in strong thermal contact with the TES. The TESs are coupled to the bath through weak thermal links. Niobium leads, which provide the voltage bias to the TES, connect to bond pads which are wire-bonded to custom inductor and capacitor (LC) boards and the rest of the FDM readout scheme. Each bolometer encodes the signal from one frequency band and one polarization and each SAMP encodes the signal from three bands and both polarizations.

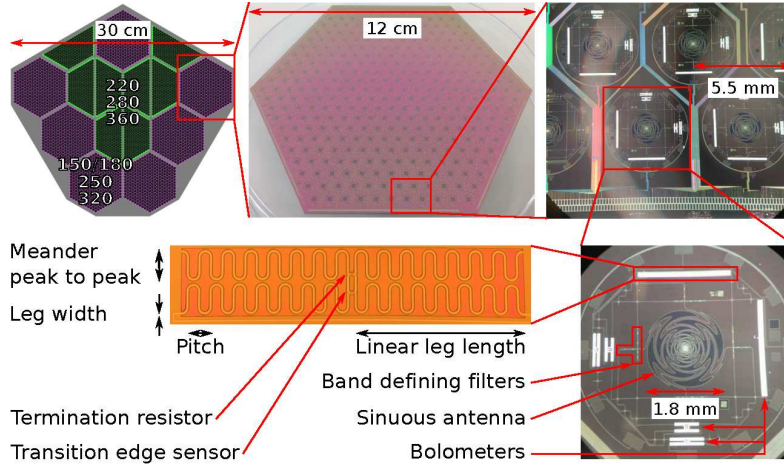


Fig. 2 *Top left*: a model of the EBEX-IDS focal plane composed of low frequency (150 or 180, 250, and 320 GHz) and high frequency pixels (220, 280, and 360 GHz). *Top center*: a picture of an EBEX-IDS bolometer wafer. *Top right*: a picture of four SAMPs. *Bottom right*: a picture of a SAMP tri-plexer pixel with straight bolometer legs. *Bottom left*: a picture of a bolometer with four distinct meandered legs.

We calculate the emission from the CMB, the emission from the atmosphere, and the transmission and emission of each of the optical elements from first principles and derive the expected power absorbed by the bolometers [3]. We calculate a value of 0.2 pW within the 150 GHz band, the frequency band for which we expect the smallest power, and include a 0.4 pW margin to conservatively account for the known challenge of assembling a cryostat to the theoretical specifications. Assuming a safety factor of 2.5, we require the EBEX-IDS bolometers observing at 150 GHz to have an average thermal conductance \bar{G} of 9 pW/K. We specify the bolometer legs to be shorter than 1.5 mm due to constraints on the physical size of the focal plane and the number of pixels. The TES of the ~ 70 pW/K bolometers designed for the ground-based telescopes POLARBEAR and SPT-3G are physically supported by four straight legs [2, 4]. In order to decrease \bar{G} , we thin and elongate these legs. We also use a meandered leg design, inspired by SPIDER, which allows for the elongation of the effective length of the legs while preserving the size of the pixel; see Figure 2 [5].

We measure the maximal power the bolometer can absorb before saturation P_{sat} , which depends on the temperature of the bath T_0 and the critical temperature of the TES T_c , by measuring the electric power required to operate the detector in the strong electrothermal feedback regime in a dark environment and calculate

$$\bar{G}(T_0, T_c) = P_{sat}(T_0, T_c)/(T_c - T_0). \quad (1)$$

A measurement of P_{sat} at various bath temperatures is shown in Figure 3. We also measure T_c by providing a small voltage bias and measuring the resistance of the TES as a function of the bath temperature [3]. We assume the thermal conductivity of the bolometer follows a power law $\kappa = \kappa_0 T^n$ and hence

$$P_{sat}(T_0, T_c) = \frac{P_{sat,0}}{n+1} (T_c^{n+1} - T_0^{n+1}), \quad (2)$$

where $P_{sat,0}$ is the theoretical saturation power at 0 K. We report the average thermal conductance in EBEX-IDS conditions, which we denote with a *. We set T_0^* to 250 mK by design and we specify T_c^* to 440 mK to minimize the contribution of the phonon noise [2]. We extract n by measuring P_{sat} at various bath temperature and we fit for $P_{sat,0}$, n and T_c . We find an average value of 2.6 for n and critical temperatures consistent with the measurement described previously.

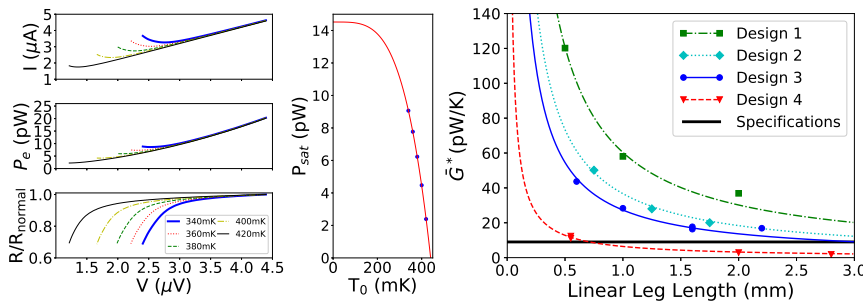


Fig. 3 *Left*: the current I , the electrical power P_e and the fraction of normal resistance R/R_{normal} measured for a bolometer while it is dropped into its superconducting transition at various bath temperatures. *Middle*: the saturation power as a function of the bath temperature (*blue circles*) fitted to the model described by Equation 2 (*red solid*). *Right*: the measured average thermal conductance extrapolated to EBEX-IDS conditions (*symbols*) with the inverse leg length fitted model (*lines*) as a function of the linear leg length for the four designs described in Table 1.

We report on four leg designs for which the characteristic dimensions are defined in Figure 2 and are quantified in Table 1. Two sets of chips with different characteristics were tested for design 4. Initial designs with only two straight legs instead of four showed mechanical instability and were not further pursued. We measure that \bar{G} is inversely proportional to the leg length and we tune \bar{G}^* using this parameter; see Figure 3. Design 4 with a projected critical temperature of 440 mK meets the 9 pW/K EBEX-IDS specifications for bolometer legs longer than 0.71 mm. The critical temperature will be decreased by reducing the fraction of aluminium in the TES during fabrication. The next design will focus on improving detector yield by implementing new release techniques to minimize the stress on the legs and by implementing small design changes to minimize asymmetries.

Finally, the optical properties of a prototype with frequency bands close to EBEX-IDS meet specifications as shown in Figure 4. We measure the transmission bands of a triplexer prototype pixel with a Fourier transform spectrometer using a ceramic heater as a thermal source. The band edges are as expected from simulations [6]. The beam is measured by translating a chopped liquid nitrogen source in an X-Y raster scan below a test cryostat and recording the response at each location.

Design	Leg type	Leg width μm	Meander peak to peak μm	Pitch μm	$P_{\text{sat}}^{\dagger\ddagger}$ pW	T_c mK	$\bar{G}^{*\ddagger}$ pW/K
1	Straight	30, 18	N/A	N/A	13	500	40
2	Straight	16	N/A	N/A	6.9	490	25
3	Meander	16	200	150	6.5	510	18
4.1	Meander	12	140	60	1.3	510	4.1
4.2	Meander	12	140	60	0.6	400	4.4

[†] corrected to T_0^*

[‡] for 1.5 mm legs

Table 1 Physical characteristics of the bolometer designs. The dimensions are defined in Figure 2. Design 1 has two $30 \mu\text{m}$ wide legs supporting the microstrip and two $18 \mu\text{m}$ wide legs supporting the bias lines. Design 4 has its ground planes removed on the two legs carrying the bias lines.

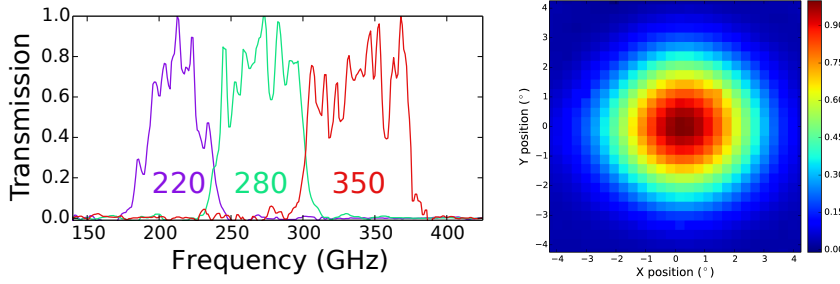


Fig. 4 *Left*: the peak-normalized transmission of a 220, 280, and 350 GHz tri-plexer pixel close to the EBEX-IDS specifications. *Right*: the beam of a 220 GHz SAMP pixel designed for POLARBEAR2 sharing the EBEX-IDS optical design [2, 6].

3 Readout

EBEX-IDS will use the latest FDM technology: the ICE boards [7]. With the FDM, we simultaneously read out a group of detectors with only 2 wires. The ICE boards support a multiplexing factor of $\times 128$ and a multiplexing factor of $\times 68$ has been demonstrated by SPT-3G using the 1.6 - 5.3 MHz frequency range. For EBEX-IDS to achieve its planned sensitivity, a multiplexing factor of $\times 105$ is required. We increase the multiplexing factor through two steps.

First, we decrease the spacing of the resonant frequencies by increasing the inductance of the band selecting inductors from $60 \mu\text{H}$ to $90 \mu\text{H}$. The crosstalk due to the mutual inductance of the inductors can be arbitrarily decreased by ensuring the LCs of neighbouring frequencies are physically far on the LC chip; see Figure 5. The magnitude of crosstalk due to voltage biases from the frequency neighbours is given by $|\frac{R}{2\Delta\omega L}|^2$. We calculate crosstalk of 0.09% (0.05%) at 0.4 MHz (5.3 MHz) with a 30 kHz (112 kHz) spacing. The magnitude of the crosstalk caused by the signal from a bolometer heating its neighbour due to voltage drop across the non-zero impedance of the wiring or the superconducting quantum interference device (SQUID) is $X_I \frac{L_{\text{stray}}}{L} \frac{\omega}{\Delta\omega}$, where X_I is the ratio between the current through bolometer $i \pm 1$ caused by bolometer i to the current through bolometer i . We calculate crosstalk of 0.05% (0.04%) at 0.4 MHz (5.3 MHz) with a 30 kHz (112 kHz) spacing and a stray inductance L_{stray} of $100 \mu\text{H}$ [8]. The electrical crosstalk remains well below the expected optical crosstalk of 1%.

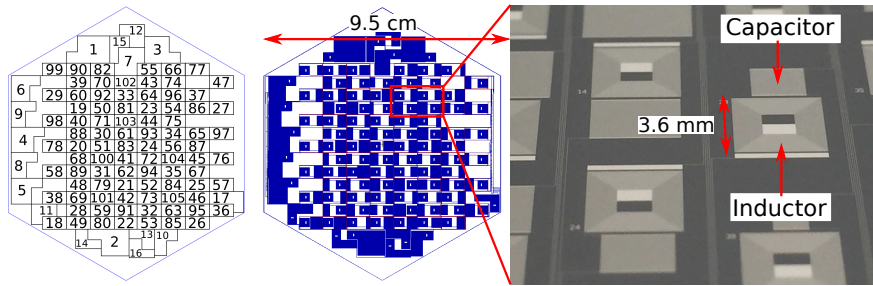


Fig. 5 *Left*: the location of the LC pairs on the LC chip. The lowest frequency is labelled “1” and the highest, “105”. *Middle*: a model of the LC chip. *Right*: a zoom on a picture of LC pairs.

Second, we extend the range of frequency used. Using frequencies above 5.3 MHz is challenging because of capacitive strays from the FDM band selecting capacitors and inductive strays from wiring; both increase with frequency. We therefore extend the frequency range towards lower frequencies to 0.4 - 5.3 MHz.

We are now developing a new LC chip fabricated with a $2\ \mu\text{m}$ lithographic process. The inductors are $3.6 \times 3.6\ \text{mm}$ squares composed of 200 turns of $3\ \mu\text{m}$ wide niobium wires also separated by $3\ \mu\text{m}$. We use 10 - 1759 pF interdigitated capacitors to define the bolometer bias frequency. Figure 5 shows the design of the EBEX-IDS chip where the 105 LC pairs are position on a hexagonal silicon wafer with 5.5 cm sides, similar in size to the hexagonal bolometer wafer with 5 cm sides. We use a frequency spacing of 30 kHz for the frequency range 0.4 - 1.5 MHz and a logarithmic spacing for the frequency range 1.6 - 5.3 MHz, which is 30 kHz at 1.5 MHz and 112 kHz at 5.3 MHz.

A hexagonal printed circuit board (PCB) mounting board for the LC chip with 6 cm sides is being designed. This board will be stacked under the bolometer wafer for compactness, hence the hexagonal shape.

4 Summary

We have fabricated and characterized bolometers that exceed the EBEX-IDS specifications. Bolometers composed of four $12\ \mu\text{m}$ wide, $140\ \mu\text{m}$ peak to peak, and $0.71\ \text{mm}$ long meandered legs with a $60\ \mu\text{m}$ pitch, as defined in Figure 2, in combination with TESs which have a 440 mK critical temperature meet the $9\ \text{pW/K}$ specified average thermal conductance. We are in the process of fabricating optical pixels for EBEX-IDS. EBEX-IDS will use the ICE boards to read out detectors in the frequency domain with a multiplexing factor 60% higher than the highest factor to date. The design of the sub-Kelvin readout components is almost completed and will soon be tested. The lower thermal conductance bolometers achieved with the meandered leg design combined with the highest FDM factor to date increases the readiness of this detectors technology for balloon platform and will allow EBEX-IDS to achieve its specified sensitivity.

Acknowledgements The EBEX-IDS Collaboration would like to thank the support from NASA (NNX17AH30G).

References

1. BICEP2/Keck Collaboration and Planck Collaboration et al., *Phys. Rev. Lett.* **114**, 101301, (2015), DOI: 10.1103/PhysRevLett.114.101301.
2. A. Suzuki, *University of California, Berkeley* (2013).
3. The EBEX Collaboration et al., *Astrophys. J.* (*in prep*).
4. C.M. Posada et al., *Proc. SPIE* **9914**, 991417, (2016), DOI: 10.1117/12.2232912.
5. A. Orlando et al., *Proc. SPIE* **7741**, 77410H, (2010), DOI: 10.1117/12.857914.
6. B. Westbrook et al., *J. Low Temp. Phys.* **184**, 74, (2016), DOI: 10.1007/s10909-016-1508-x.
7. A.N. Bender et al., *Proc. SPIE* **9153**, page91531A, (2014), DOI: 10.1117/12.2054949.
8. M.A. Dobbs et al., *Rev. Sci. Instrum.* **83**, 073113, (2012), DOI: 10.1063/1.4737629.